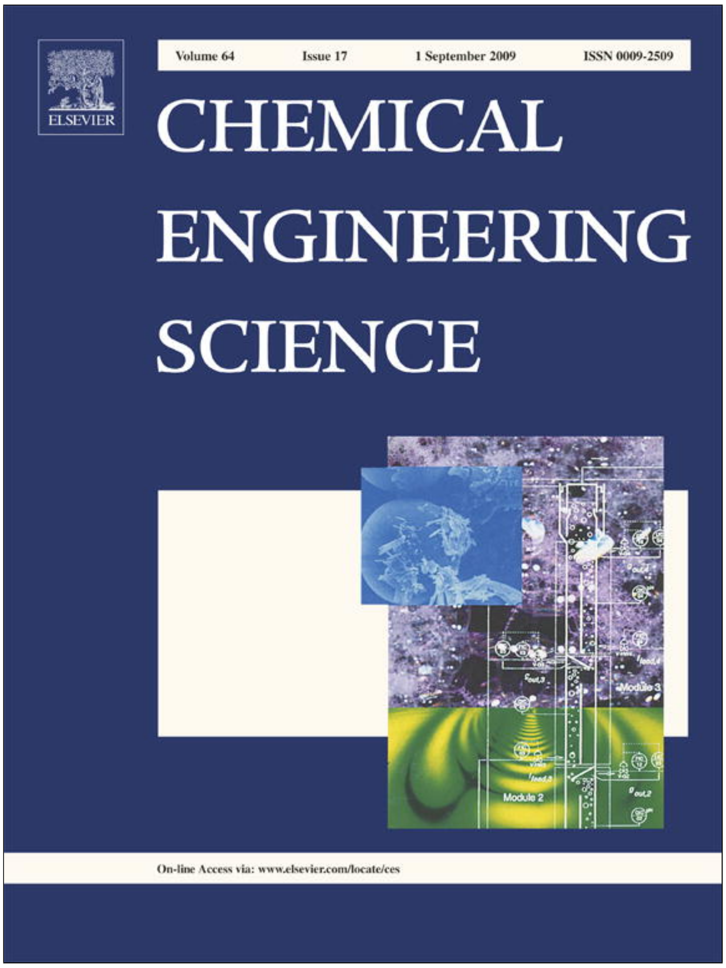

Volume 64 Issue 17 1 September 2009 ISSN 0009-2509

CHEMICAL ENGINEERING SCIENCE

On-line Access via: www.elsevier.com/locate/ces

Chemical Engineering Science 64 (2009) 3903–3913

Contents lists available at ScienceDirect

Chemical Engineering Science

journal homepage: www.elsevier.com/locate/ces

Regulation of film thickness, surface roughness and porosity in thin film growth using deposition rate

Gangshi Hu[a], Gerassimos Orkoulas[a], Panagiotis D. Christofides[a,b,*]

[a]Department of Chemical and Biomolecular Engineering, University of California, Los Angeles, CA 90095, USA
[b]Department of Electrical Engineering, University of California, Los Angeles, CA 90095, USA

ARTICLE INFO

Article history:
Received 7 April 2009
Received in revised form 19 May 2009
Accepted 20 May 2009
Available online 30 May 2009

Keywords:
Model predictive control
Stochastic PDEs
Thin film growth
Process control
Process simulation
Process optimization

ABSTRACT

This work focuses on distributed control of film thickness, surface roughness and porosity in a porous thin film deposition process using the deposition rate as the manipulated input. The deposition process includes adsorption and migration processes and it is modeled via kinetic Monte Carlo simulation on a triangular lattice with vacancies and overhangs allowed to develop inside the film. A distributed parameter (partial differential equation) dynamic model is derived to describe the evolution of the surface height profile of the thin film accounting for the effect of deposition rate. The dynamics of film porosity, evaluated as film site occupancy ratio, are described by an ordinary differential equation. The developed dynamic models are then used as the basis for the design of a model predictive control algorithm that includes penalty on the deviation of film thickness, surface roughness and film porosity from their respective set-point values. Simulation results demonstrate the applicability and effectiveness of the proposed modeling and control approach in the context of the deposition process under consideration.

1. Introduction

Modeling and control of thin film microstructure in thin film deposition processes has attracted significant research attention in recent years. Specifically, kinetic Monte Carlo (kMC) models based on a square lattice and utilizing the solid-on-solid (SOS) approximation for deposition were initially employed to describe the evolution of film microstructure and design feedback control laws for thin film surface roughness (Lou and Christofides, 2003a; Siettos et al., 2003; Reese et al., 2001; Christofides et al., 2008). Furthermore, a method that couples partial differential equation (PDE) models and kMC models was developed for computationally efficient multiscale optimization of thin film growth (Varshney and Armaou, 2005, 2008a,b). However, kMC models are not available in closed form and this limitation restricts the use of kMC models for system-level analysis and design of model-based feedback control systems.

Stochastic differential equations (SDEs) arise naturally in the modeling of surface morphology of ultrathin films in a variety of thin film preparation processes (Edwards and Wilkinson, 1982; Villain, 1991; Vvedensky et al., 1993; Cuerno et al., 1995; Lauritsen et al., 1996). Advanced control methods based on SDEs have been developed to address the need of model-based feedback control of thin film microstructure. Specifically, methods for state/output feedback control of surface roughness based on linear (Ni and Christofides, 2005) and nonlinear (Lou et al., 2008) SDE models have been developed; the reader may refer to (Christofides et al., 2008) for detailed results and extensive reference lists.

In the context of modeling of thin film porosity, kMC models have been widely used to model the evolution of porous thin films in many deposition processes (Wang and Clancy, 1998, 2001; Zhang et al., 2004; Levine and Clancy, 2000). With respect to porosity modeling for control, deterministic and stochastic ordinary differential equation (ODE) models of film porosity were recently developed (Hu et al., 2009a) to model the evolution of film porosity and its fluctuation and design model predictive control (MPC) algorithms to control film porosity to a desired level and reduce run-to-run porosity variability. In MPC, the optimal manipulated input is obtained from the solution of an on-line optimization problem which minimizes a cost function that penalizes the errors from the set-points at designated finite horizons. MPC is widely used in the control of many chemical processes due to its capability to handle input and state constraints and its robustness against model uncertainty and external disturbances (Mayne et al., 2000; Christofides and El-Farra, 2005). Simultaneous regulation of film surface roughness and porosity within a unified MPC framework was also recently investigated (Hu et al., 2009b) using the substrate temperature as the

---

[*] Corresponding author at: Department of Chemical and Biomolecular Engineering, University of California, Los Angeles, CA 90095, USA. Tel.: +1 310794 1015; fax: +1 310206 4107.
E-mail address: pdc@seas.ucla.edu (P.D. Christofides).

0009-2509/$ - see front matter © 2009 Elsevier Ltd. All rights reserved.
doi:10.1016/j.ces.2009.05.034

manipulated input (Hu et al., 2009a,b). However, the weak dependence of the film thickness on the substrate temperature does not allow regulation of the film thickness at the end of the deposition process by manipulation of the substrate temperature. A good manipulated input candidate for the control of film thickness (Lou and Christofides, 2003b) (and for film surface roughness and porosity as well) is the deposition rate, which has a direct influence on the growth rate of the film. At this stage, a careful look of the existing literature indicates that the simultaneous control of film surface roughness, thickness and porosity by manipulating the deposition rate remains still an unresolved issue.

Motivated by these considerations, this work focuses on distributed control of film thickness, surface roughness and porosity in a porous thin film deposition process using the deposition rate as the manipulated input. The deposition process includes adsorption and migration processes and it is modeled via kinetic Monte Carlo simulation on a triangular lattice with vacancies and overhangs allowed to develop inside the film. A distributed parameter (partial differential equation) dynamic model is derived to describe the evolution of the surface height profile of the thin film accounting for the effect of deposition rate. The dynamics of film porosity, evaluated as film site occupancy ratio, are described by an ordinary differential equation. The developed dynamic models are then used as the basis for the design of a model predictive control algorithm that includes penalty on the deviation of film thickness, surface roughness and film porosity from their respective set-point values. Simulation results demonstrate the applicability and effectiveness of the proposed modeling and control approach in the context of the deposition process under consideration.

2. Preliminaries

2.1. On-lattice kinetic Monte Carlo model of film growth

The deposition process is simulated using an on-lattice kMC model which is constructed on a two-dimensional triangular lattice (one dimensional on the growth direction) (Hu et al., 2009b), as shown in Fig. 1. The on-lattice kMC model is valid for a low temperature region, $T < 0.5T_m$ (T_m is the melting point of the crystalline material), where the particles can be assumed to be constrained on the lattice sites (Wang and Clancy, 1998). The lattice contains a fixed number of sites in the lateral direction. Two microscopic processes are included in the kMC model: an adsorption process, in which particles are incorporated into the film from the gas phase, and a migration process, in which surface particles move to adjacent sites (Wang and Clancy, 1998, 2001; Levine and Clancy, 2000; Yang et al., 1997). The new particles are always deposited from the gas phase which is located above the lattice; see Fig. 1. The growth direction, along which the thin film keeps growing, is normal to the lateral direction. The number of sites in the lateral direction is defined as the lattice size and is denoted by L. The lattice parameter, a, which is defined as the distance between two neighboring sites and equals the diameter of a particle (all particles have the same diameter), determines the lateral extent of the lattice, La.

The number of nearest neighbors of a site ranges from zero to six, the coordination number of the triangular lattice. A site with no nearest neighbors indicates an unadsorbed particle in the gas phase (i.e., a particle which has not been deposited on the film yet). A particle with six nearest neighbors is associated with an interior particle that is fully surrounded by other particles and cannot migrate. A particle with one to five nearest neighbors is possible to diffuse to an unoccupied neighboring site with a probability that depends on its local environment. In the triangular lattice, a particle with only one nearest neighbor is considered unstable and is subject to instantaneous surface relaxation. Details of particle surface relaxation and migration will be discussed in Sections 2.2 and 2.3 below.

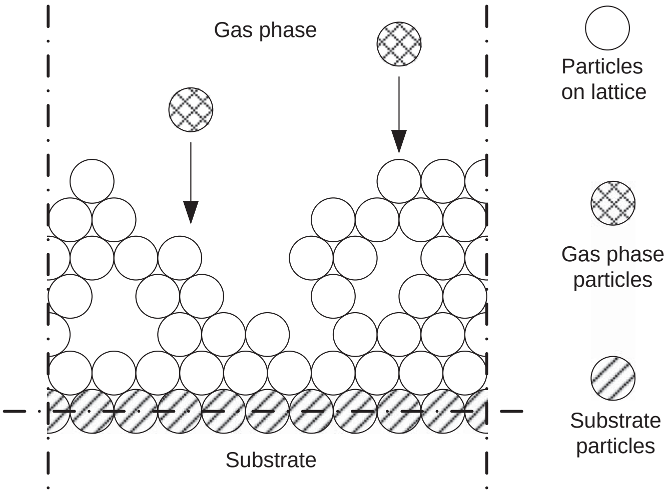

Fig. 1. Thin film growth process on a triangular lattice.

In the simulation, a bottom layer in the lattice is initially set to be fully packed and fixed, as shown in Fig. 1. There are no vacancies in this layer and the particles in this layer cannot migrate. This layer acts as the substrate for the deposition and is not counted in the computation of the number of the deposited particles, i.e., this fixed layer does not influence the film porosity (see Section 2.4 below). Two types of microscopic processes (Monte Carlo events) are considered: an adsorption process, in which particles are incorporated into the film from the gas phase, and a migration process, in which surface particles move to adjacent sites (Wang and Clancy, 1998, 2001; Levine and Clancy, 2000; Yang et al., 1997). These Monte Carlo events are assumed to be Poisson processes. All events occur randomly with probabilities proportional to their respective rates. The events are executed instantaneously upon selection and the state of the lattice remains unchanged between two consecutive events.

2.2. Adsorption process

In an adsorption process, an incident particle comes in contact with the film and is incorporated onto the film. The microscopic adsorption rate, W, which is in units of layers per unit time, depends on the gas phase concentration. The layers in the unit of adsorption rate are densely packed layers, which contain L particles. With this definition, W is independent of L. In this work, the macroscopic adsorption rate (deposition rate), W, is treated as a process parameter and will be used as the manipulated input. For the entire deposition process, the microscopic adsorption rate (deposition rate) in terms of incident particles per unit time, which is denoted as r_a, is related to W as follows:

$$r_a = LW \tag{1}$$

The incident particles are initially placed at random positions above the film lattice and move toward the lattice in the vertical direction. The random initial particle position, x_0, which is the center of an incident particle, follows a uniform probability distribution in the continuous domain, $(0, La)$. Different distributions of the incident angle may be selected, e.g., a uniform or cosine distribution, for different film growth processes (Hu et al., 2009a; Yang et al., 2005). In this work, a Dirac delta distribution function of incident angle (deterministic incident angle) is used for vertical incidence.

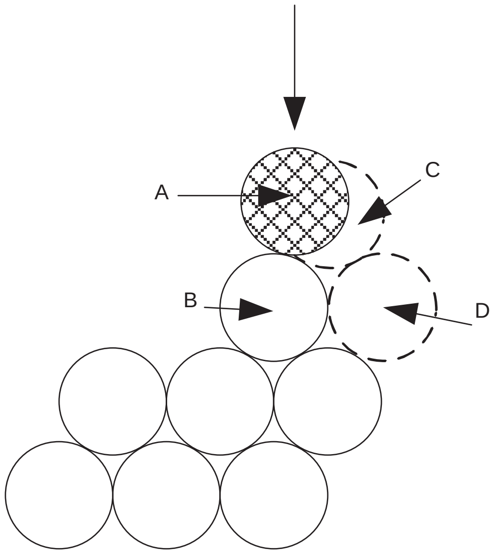

Fig. 2. Schematic of the adsorption event with surface relaxation. In this event, particle A is the incident particle, particle B is the surface particle that is first hit by particle A, site C is the nearest vacant site to particle A among the sites that neighbor particle B and site D is a stable site where particle A relaxes.

The procedure of an adsorption process is illustrated in Fig. 2. After the initial position is determined, the incident particle, A, travels along a straight line towards the film until contacting the first particle, B, on the film. Upon contact, particle A stops and sticks to particle B at the contacting position; see Fig. 2. Then, particle A moves (relaxes) to the nearest vacant site, C, among the neighboring sites of particle B. Surface relaxation is conducted if site C is unstable, i.e., site C has only one neighboring particle, as shown in Fig. 2. When a particle is subject to surface relaxation, the particle moves to its most stable neighboring vacant site, which is defined as the site with the most nearest neighbors. In the case of multiple neighboring vacant sites with the same number of nearest neighbors, a random one is chosen from these sites with equal probability as the objective of the particle surface relaxation process. Note that particle surface relaxation is considered as part of the deposition event, and thus, it does not contribute to the process simulation time. There is also only one relaxation event per incident particle.

2.3. Migration process

In a migration process, a particle overcomes the energy barrier of the site and jumps to its vacant neighboring site. The migration rate (probability) of a particle follows an Arrhenius-type law with a pre-calculated activation energy barrier that depends on the local environment of the particle, i.e., the number of the nearest neighbors of the particle chosen for a migration event. The migration rate of the ith particle is calculated as follows:

$$r_{m,i} = \nu_0 \exp\left(-\frac{n_i E_0}{k_B T}\right) \tag{2}$$

where ν_0 denotes the pre-exponential factor, n_i is the number of the nearest neighbors of the ith particle and can take the values of 2, 3, 4 and 5 ($r_{m,i}$ is zero when $n_i = 6$ since this particle is fully surrounded by other particles and cannot migrate), E_0 is the contribution to the activation energy barrier from each nearest neighbor, k_B is the Boltzmann's constant and T is the substrate temperature of the thin film. Since the film is thin, the temperature is assumed to be uniform throughout the film and is treated as a time-varying but spatially invariant process parameter. In this work, the factor and energy barrier contribution in Eq. (2) take the following values $\nu_0 = 10^{13}\,\mathrm{s}^{-1}$ and $E_0 = 0.9\,\mathrm{eV}$. These values are appropriate for a silicon film (Keršulis and Mitin, 1995). Here we note that the contributions to the activation energy barrier from the second nearest neighbors are added into the contributions from the nearest neighbors. When a particle is subject to migration, it can jump to either of its vacant neighboring sites with equal probability, unless the vacant neighboring site has no nearest neighbors, i.e., the surface particle cannot jump off the film and it can only migrate on the surface.

The deposition process is simulated using an approach based on the continuous-time Monte Carlo (CTMC) method. CTMC method (Vlachos et al., 1993) is advantageous compared to the null-event algorithm (Ziff et al., 1986) in the context of closed-to-zero rates of the events in the Monte Carlo simulations. The null-event algorithm tries to execute Monte Carlo events on randomly selected sites with certain probabilities, which is suitable for simulations of SOS models. However, the continuous-time CTMC method selects an event before the selection of the site on which the event is going to be executed. In the CTMC method, all microscopic processes are assumed to be Poisson processes. A complete event list is created at the beginning and is updated based on the current state of the lattice after an event, i.e., deposition process or migration process, is selected and executed. The time increment upon the execution of a successful event is computed based on the total rates of all possible events that are included in the event list. Details of the simulation algorithm and discussion can be found in Hu et al. (2009a).

2.4. Definitions of surface height profile and film site occupancy ratio

Utilizing the continuous-time Monte Carlo algorithm, simulations of the kMC model of a porous silicon thin film growth process can be carried out. Snapshots of film microstructure, i.e., the configurations of particles within the triangular lattice, are obtained from the kMC model at various time instants during process evolution. To quantitatively evaluate the thin film microstructure, two variables, surface roughness and film porosity, are introduced in this subsection.

Surface roughness, which measures the texture of thin film surface, is represented by the root mean square (RMS) of the surface height profile of the thin film. Determination of surface height profile is slightly different in the triangular lattice model compared to a solid-on-solid model. In the SOS model, the surface of thin film is naturally described by the positions of the top particles of each column. In the triangular lattice model, however, due to the existence of vacancies and overhangs, the definition of film surface needs further clarification. Specifically, taking into account practical considerations of surface roughness measurements, the surface height profile of a triangular lattice model is defined based on the particles that can be reached in the vertical direction, as shown in Fig. 3. In this definition, a particle is considered as a surface particle only if it is not blocked by the particles in the neighboring columns. Therefore, the surface height profile of a porous thin film is the line that connects the sites that are occupied by the surface particles. With this definition, the surface height profile can be treated as a function of the spatial coordinate. Surface roughness, as a measurement of the surface texture, is defined as the standard deviation of the surface height profile from its average height. The definition expression of surface roughness is given later in Section 3.1.

In addition to film surface roughness, the film site occupancy ratio (SOR) is introduced to represent the extent of the porosity inside the thin film. The mathematical expression of film SOR is defined as

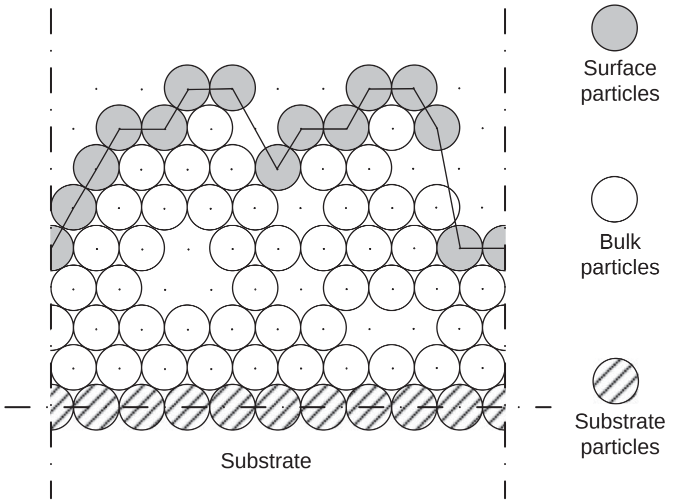

Fig. 3. Definition of surface height profile. A surface particle is a particle that is not blocked by particles from both of its neighboring columns in the vertical direction.

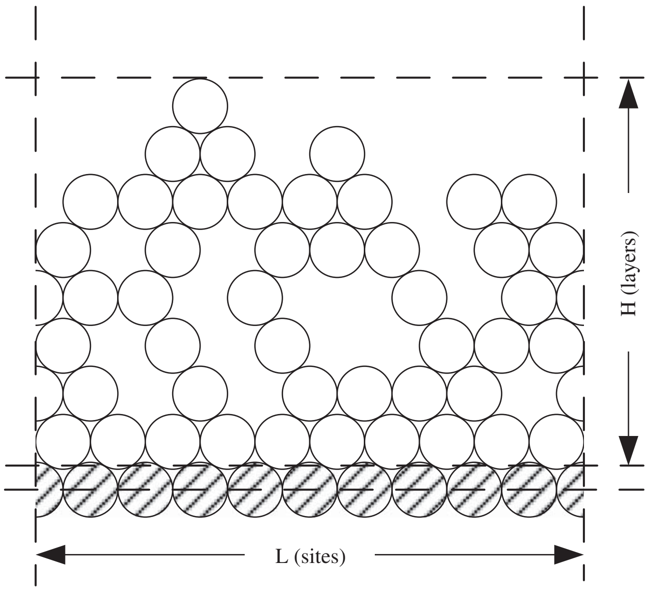

Fig. 4. Illustration of the definition of film SOR of Eq. (3).

follows:

$$\rho = \frac{N}{LH} \tag{3}$$

where ρ denotes the film SOR, N is the total number of deposited particles on the lattice, L is the lattice size and H denotes the number of deposited layers. Note that the deposited layers are the layers that contain only deposited particles and do not include the initial substrate layers. The variables in the definition expression of Eq. (3) can be found in Fig. 4. Since each layer contains L sites, the total number of sites in the film that can be contained within the H layers is LH. Thus, film SOR is the ratio of the occupied lattice sites, N, over the total number of available sites, LH. Film SOR ranges from 0 to 1. Specifically, $\rho = 1$ denotes a fully occupied film with a flat surface. The value of zero is assigned to ρ at the beginning of the deposition process since there are no particles deposited on the lattice.

The definition of film SOR is different from the concept of packing density which is used to denote the fraction of a volume filled by a given collection of solids, and thus, packing density cannot be used to characterize the evolution of the porosity. Another important point is the correlation of film surface roughness and film porosity. These two properties of thin films are correlated to some extent in the deposition process. The conditions that produce a dense film, i.e., higher substrate temperature or lower deposition rate, also generate a smoother surface. However, even though there is correlation between the film surface roughness and porosity, films with the same surface roughness may have quite different film SORs.

3. Dynamic model construction and parameter estimation

3.1. Edwards–Wilkinson-type equation of surface height using deposition rate as manipulated input

An Edwards–Wilkinson (EW)-type equation, a second-order stochastic partial differential equation, can be used to describe the surface height evolution in many microscopic processes that involve thermal balance between adsorption (deposition) and migration (diffusion) (Lou and Christofides, 2005). In this work, an EW-type equation is chosen to describe the dynamics of the fluctuation of surface height (the validation of this choice will be made clear below) of the form:

$$\frac{\partial h}{\partial t} = r_h + v\frac{\partial^2 h}{\partial x^2} + \xi(x,t) \tag{4}$$

subject to PBCs:

$$h(-\pi,t) = h(\pi,t), \quad \frac{\partial h}{\partial x}(-\pi,t) = \frac{\partial h}{\partial x}(\pi,t) \tag{5}$$

and the initial condition:

$$h(x,0) = h_0(x) \tag{6}$$

where $x \in [-\pi,\pi]$ is the spatial coordinate, t is the time, r_h and v are the model parameters and $\xi(x,t)$ is a Gaussian white noise with the following mean and covariance:

$$\langle \xi(x,t) \rangle = 0$$
$$\langle \xi(x,t)\xi(x',t') \rangle = \sigma^2 \delta(x-x')\delta(t-t') \tag{7}$$

where σ^2 is a parameter which measures the intensity of the Gaussian white noise and $\delta(\cdot)$ denotes the standard Dirac delta function. We note that the parameters r_h, v and σ^2 are functions of the deposition rate, W, and this dependence will be estimated and discussed in Section 3.3 below.

To proceed with model parameter estimation and control design, a stochastic ODE approximation of Eq. (4) is first derived using model decomposition. Consider the eigenvalue problem of the linear operator of Eq. (4), which takes the form:

$$A\bar{\phi}_n(x) = v\frac{d^2\bar{\phi}_n(x)}{dx^2} = \lambda_n \bar{\phi}_n(x)$$
$$\bar{\phi}_n(-\pi) = \bar{\phi}_n(\pi), \quad \frac{d\bar{\phi}_n}{dx}(-\pi) = \frac{d\bar{\phi}_n}{dx}(\pi) \tag{8}$$

where λ_n denotes an eigenvalue and $\bar{\phi}_n$ denotes an eigenfunction. A direct computation of the solution of the above eigenvalue problem yields $\lambda_0 = 0$ with $\psi_0 = 1/\sqrt{2\pi}$, and $\lambda_n = -vn^2$ (λ_n is an eigenvalue of multiplicity two) with eigenfunctions $\phi_n = (1/\sqrt{\pi})\sin(nx)$ and $\psi_n = (1/\sqrt{\pi})\cos(nx)$ for $n = 1,\ldots,\infty$. Note that the $\bar{\phi}_n$ in Eq. (8) denotes either ϕ_n or ψ_n. For a fixed positive value of v, all eigenvalues (except the zeroth eigenvalue) are negative and the distance between two consecutive eigenvalues (i.e., λ_n and λ_{n+1}) increases as n increases.

The solution of Eq. (4) is expanded in an infinite series in terms of the eigenfunctions of the operator of Eq. (8) as follows:

$$h(x,t)=\sum_{n=1}^{\infty}\alpha_n(t)\phi_n(x)+\sum_{n=0}^{\infty}\beta_n(t)\psi_n(x) \tag{9}$$

where $\alpha_n(t)$, $\beta_n(t)$ are time-varying coefficients. Substituting the above expansion for the solution, $h(x,t)$, into Eq. (4) and taking the inner product with the adjoint eigenfunctions, $\phi_n^*(x)=(1/\sqrt{\pi})\sin(nx)$ and $\psi_n^*(x)=(1/\sqrt{\pi})\cos(nx)$, the following system of infinite stochastic ODEs is obtained:

$$\begin{aligned}
&\frac{d\beta_0}{dt}=\sqrt{2\pi}r_h+\xi_\beta^0(t)\\
&\frac{d\alpha_n}{dt}=\lambda_n\alpha_n+\xi_\alpha^n(t),\quad n=1,\ldots,\infty\\
&\frac{d\beta_n}{dt}=\lambda_n\beta_n+\xi_\beta^n(t),\quad n=1,\ldots,\infty
\end{aligned} \tag{10}$$

where

$$\xi_\alpha^n(t)=\int_{-\pi}^{\pi}\xi(x,t)\phi_n^*(x)\,dx,\quad \xi_\beta^n(t)=\int_{-\pi}^{\pi}\xi(x,t)\psi_n^*(x)\,dx \tag{11}$$

The covariances of $\xi_\alpha^n(t)$ and $\xi_\beta^n(t)$ can be obtained: $\langle\xi_\alpha^n(t)\xi_\alpha^n(t')\rangle=\sigma^2\delta(t-t')$ and $\langle\xi_\beta^n(t)\xi_\beta^n(t')\rangle=\sigma^2\delta(t-t')$. Due to the orthogonality of the eigenfunctions of the operator in the EW equation of Eq. (4), $\xi_\alpha^n(t)$ and $\xi_\beta^n(t)$, $n=0,1,\ldots$, are stochastically independent.

Since the stochastic ODE system is linear, the analytical solution of state variance can be obtained from a direct computation as follows:

$$\begin{aligned}
&\langle\alpha_n^2(t)\rangle=\frac{\sigma^2}{2\nu n^2}+\left(\langle\alpha_n^2(t_0)\rangle-\frac{\sigma^2}{2\nu n^2}\right)e^{-2\nu n^2(t-t_0)}\\
&\langle\beta_n^2(t)\rangle=\frac{\sigma^2}{2\nu n^2}+\left(\langle\beta_n^2(t_0)\rangle-\frac{\sigma^2}{2\nu n^2}\right)e^{-2\nu n^2(t-t_0)}\\
&\quad n=1,2,\ldots,\infty
\end{aligned} \tag{12}$$

where $\langle\alpha_n^2(t_0)\rangle$ and $\langle\beta_n^2(t_0)\rangle$ are the state variances at time t_0. The analytical solution of state variance of Eq. (12) will be used in the parameter estimation and the MPC design.

When the dynamic model of surface height profile is determined, surface roughness of the thin film is defined as the standard deviation of the surface height profile from its average height and is computed as follows:

$$r(t)=\sqrt{\frac{1}{2\pi}\int_{-\pi}^{\pi}[h(x,t)-\bar{h}(t)]^2\,dx} \tag{13}$$

where $\bar{h}(t)=(1/2\pi)\int_{-\pi}^{\pi}h(x,t)\,dx$ is the average surface height. According to Eq. (9), we have $\bar{h}(t)=\beta_0(t)\psi_0$. Therefore, $\langle r^2(t)\rangle$ can be rewritten in terms of $\langle\alpha_n^2(t)\rangle$ and $\langle\beta_n^2(t)\rangle$ as follows:

$$\begin{aligned}
\langle r^2(t)\rangle&=\frac{1}{2\pi}\left\langle\int_{-\pi}^{\pi}(h(x,t)-\bar{h}(t))^2\,dx\right\rangle\\
&=\frac{1}{2\pi}\left\langle\sum_{i=1}^{\infty}(\alpha_i^2(t)+\beta_i^2(t))\right\rangle=\frac{1}{2\pi}\sum_{i=1}^{\infty}[\langle\alpha_i^2(t)\rangle+\langle\beta_i^2(t)\rangle]
\end{aligned} \tag{14}$$

Thus, Eq. (14) provides a direct link between the state variance of the infinite stochastic ODEs of Eq. (10) and the expected surface roughness of the thin film. Note that the parameter r_h does not appear in the expression of surface roughness, since only the zeroth state, β_0, is affected by r_h but this state is not included in the computation of the expected surface roughness square of Eq. (14).

Film thickness, which is represented by the average of surface height, $\bar{h}$, is another control objective in this work. The dynamics of the expected value of average surface height can be obtained from the analytical solution of the zeroth state, β_0, from Eq. (10), as follows:

$$\frac{d\langle\bar{h}\rangle}{dt}=r_h \tag{15}$$

subject to the initial condition

$$\langle\bar{h}(t_0)\rangle=\frac{1}{2\pi}\int_{-\pi}^{\pi}h(x,t_0)\,dx \tag{16}$$

Here we need to point out that full knowledge of surface height profile throughout the spatial domain is necessary for the computation of the initial values of the film thickness, $\langle\bar{h}(t_0)\rangle$.

Eq. (15) implies that $\bar{h}$ can be directly controlled by manipulating the deposition rate. Finally, the analytical solution of expected value of film thickness, $\langle\bar{h}\rangle$, which will be used for parameter estimation (r_h dependence on W) and control purposes below, can be obtained directly from Eq. (15) as follows:

$$\langle\bar{h}(t)\rangle=\langle\bar{h}(t_0)\rangle+r_h(t-t_0) \tag{17}$$

3.2. Dynamic model of film site occupancy ratio

Film site occupancy ratio is used to characterize film porosity. According to the definition of film SOR of Eq. (3), film SOR accounts for all deposited layers during the entire deposition process. Thus, film SOR is a cumulative property, the evolution of which can be characterized by an integral form. Before further derivation of the dynamic model of film SOR, a concept of instantaneous film SOR of the film layers deposited between time t and $t+\Delta t$, denoted by ρ_d, is first introduced as the spatial derivative of the number of deposited particles in the growing direction as follows:

$$\rho_d=\frac{dN}{d(HL)} \tag{18}$$

In Eq. (18), the lattice size L is a constant and the derivative dH can be written as a linear function of time derivative dt as follows:

$$dH=r_H\,dt \tag{19}$$

where r_H is the growth rate of the thin film from the top layer point of view. Note that r_H is different from the model coefficient r_h in Eq. (4). Thus, the expressions of N and H can be obtained by integrating Eqs. (18) and (19) as follows:

$$\begin{aligned}
&N(t)=L\int_0^t\rho_d r_H\,ds\\
&H(t)=\int_0^t\rho_d\,ds
\end{aligned} \tag{20}$$

With the definition of ρ of Eq. (3) and the expressions of N and H of Eq. (20), the film SOR of Eq. (3) can be rewritten in an integral form as follows:

$$\rho=\frac{\int_0^t\rho_d r_H\,ds}{\int_0^t r_H\,ds} \tag{21}$$

To simplify the subsequent development and develop an SOR model that is suitable for control purposes, we assume (this assumption will be verified in the closed-loop simulation results below where the performance of the controller will be evaluated) that the dynamics of the instantaneous film SOR, ρ_d, can be approximated by a first-order process, i.e.:

$$\tau\frac{d\rho_d(t)}{dt}=\rho_d^{ss}-\rho_d(t) \tag{22}$$

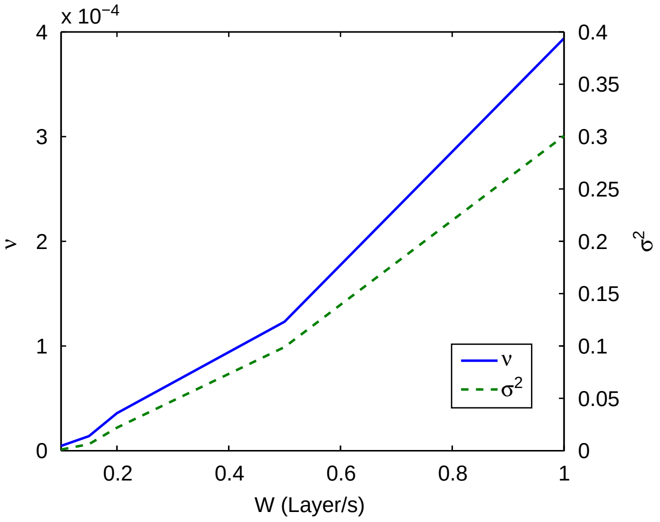

Fig. 5. Dependence of v and σ^2 on the deposition rate with substrate temperature $T=850\,\mathrm{K}$.

where τ is the time constant and ρ_d^{ss} is the steady-state value of the instantaneous film SOR. We note that the first-order ODE model of Eq. (22) was introduced and justified with numerical results in (Hu et al., 2009a) for the modeling of the partial film SOR, which is defined to characterize the evolution of the film porosity of layers that are close to the film surface. In this work, the instantaneous film SOR is a similar concept to the partial film SOR, because it also describes the contribution to the bulk film porosity of the newly deposited layers. Therefore, the first-order ODE model is a suitable choice to describe the evolution of the instantaneous film SOR.

From Eq. (21), it follows that at large times as ρ_d approaches ρ_d^{ss}, the steady-state film SOR (ρ^{ss}) approaches the steady-state value of the instantaneous film SOR (i.e., $\rho^{ss}=\rho_d^{ss}$). The deterministic ODE system of Eq. (22) is subject to the following initial condition:

$$\rho_d(t_0)=\rho_{d0} \tag{23}$$

where t_0 is the initial time and ρ_{d0} is the initial value of the instantaneous film SOR. From Eqs. (22) and (23) and the fact that $\rho^{ss}=\rho_d^{ss}$ at large times, it follows that

$$\rho_d(t)=\rho^{ss}+(\rho_{d0}-\rho^{ss})e^{-(t-t_0)/\tau} \tag{24}$$

For controller implementation purposes, the expression of the film SOR can be derived as follows:

$$\rho(t)=\frac{\int_0^{t_0}\rho_d r_H\,ds+\int_{t_0}^{t}\rho_d r_H\,ds}{\int_0^{t_0} r_H\,ds+\int_{t_0}^{t} r_H ds}=\frac{\rho(t_0)H(t_0)+\int_{t_0}^{t}\rho_d r_H\,ds}{H(t_0)+\int_{t_0}^{t} r_H\,ds} \tag{25}$$

where t_0 is the current time, $\rho(t_0)$ and $H(t_0)$ are film SOR and film height at time t_0, respectively.

Substituting the solution of ρ_d of Eq. (24) into Eq. (25) and assuming that r_H is constant for $t>\tau>t_0$, which is taken to be the case in the parameter estimation and the MPC formulations below, the analytical solution of film SOR at time t can be obtained as follows:

$$\rho=\frac{\rho(t_0)H(t_0)+r_H[\rho^{ss}(t-t_0)+(\rho^{ss}-\rho(t_0))\tau(e^{-(t-t_0)/\tau}-1)]}{H(t_0)+r_H(t-t_0)} \tag{26}$$

which is directly utilized in the model predictive control formulation of Eq. (29) below.

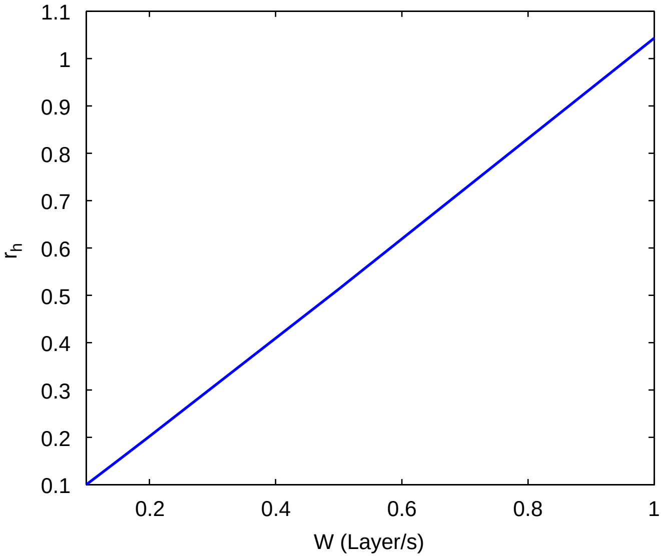

Fig. 6. Dependence of r_h on the deposition rate with substrate temperature $T=850\,\mathrm{K}$.

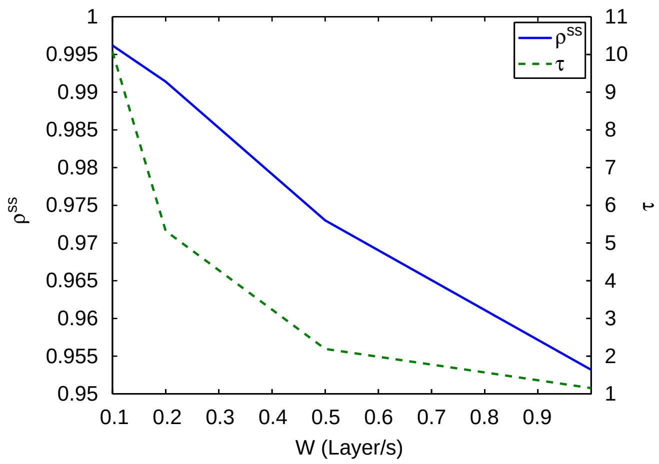

Fig. 7. Dependence of ρ^{ss} and τ on the deposition rate with substrate temperature $T=850\,\mathrm{K}$.

3.3. Parameter estimation

In the dynamic models of Eqs. (4), (15) and (22), there are five model parameters that need to be obtained from kMC data of the deposition process. These model parameters can be estimated on the basis of the open-loop simulation data at fixed operation conditions, i.e., substrate temperature and deposition rate, from the kMC model introduced in Section 2 by using least-square methods (Hu et al., 2009a,b). In the parameter estimation, the predicted evolution profiles from the dynamic models and the ones from the kMC simulation of the deposition process are compared in a least-square sense to find the best model parameters.

Different operating conditions strongly affect the deposition process and result in different dynamics of the surface height profile and of the film SOR. Thus, the model parameters are functions of the operating conditions. In this work, we choose the deposition rate, W, as the manipulated input and keep the substrate temperature fixed at $T=850\,\mathrm{K}$. The dependence of the model parameters on the deposition rate, W, can be obtained by performing the parameter estimation procedure discussed above for a variety of deposition rate values (ranging from 0.1 to 1 layer/s); see Figs. 5–7 for the dependence of the model parameters on the deposition rate. Simulation results from 1000 independent simulation runs are used for the parameter estimation under each deposition rate condition. It can be clearly seen that the model parameters are strong functions of the deposition rate and this dependence is the basis for using W to simultaneously control film thickness, roughness and porosity.

4. Model predictive controller design

In this section, a model predictive controller is designed based on the dynamic models of surface height and film SOR to regulate the expected values of surface roughness and film SOR to desired levels by manipulating the deposition rate. A desired minimum of film thickness is also included in the cost function in the MPC formulation. A reduced-order model of EW equation is used in the MPC formulation to approximate the dynamics of the surface roughness. The surface height profile and the value of film SOR are assumed to be available to the controller. In practice, these data can be obtained from in situ gas phase and thin film surface measurements (on-line film porosity may be obtained by a model that links the off-line film porosity and in situ gas phase measurements).

With respect to the choice of MPC for the controller design, we note that classical control schemes like proportional-integral (PI) control cannot be designed to explicitly account for input/state constraints, optimality considerations and the batch nature of the deposition process. Furthermore, dynamic open-loop optimization may be used but it does not provide robustness against model inaccuracies and fluctuations in the deposition process. In the case where feedback control cannot be attained, dynamic open-loop optimization may be used instead to regulate W; this is naturally included in the MPC framework employed here. The robustness of the MPC approach against model parameter uncertainty can be also improved by including adaptation schemes; see Bohm et al. (1998) and Krstic and Smyshlyaev (2008) for results on adaptive control of PDEs.

4.1. Reduced-order model for surface roughness

In model predictive control formulation, the expected surface roughness is computed from the EW equation of Eq. (4). The EW equation, which is a distributed parameter dynamic model, contains infinite dimensional stochastic states. Therefore, it leads to a model predictive controller of infinite order that cannot be realized in practice (i.e., the practical implementation of a control algorithm based on such an system will require the computation of infinite sums which cannot be done by a computer). To this end, a reduced-order model of the infinite dimensional ODE model of Eq. (10) is instead included and is used to calculate the prediction of expected surface roughness in the model predictive controller.

Due to the structure of the eigenspectrum of the linear operator of the EW equation of Eq. (4), the dynamics of the EW equation are characterized by a finite number of dominant modes. By neglecting the high-order modes ($n \geq m+1$), the system of Eq. (10) can be approximated by a finite-dimensional system as follows:

$$\frac{d\alpha_n}{dt} = \lambda_n \alpha_n + \xi_\alpha^n(t)$$
$$\frac{d\beta_n}{dt} = \lambda_n \beta_n + \xi_\beta^n(t)$$
$$n = 1, \ldots, m \qquad (27)$$

Note that the ODE for the zeroth state is also neglected, since the zeroth state does not contribute to surface roughness.

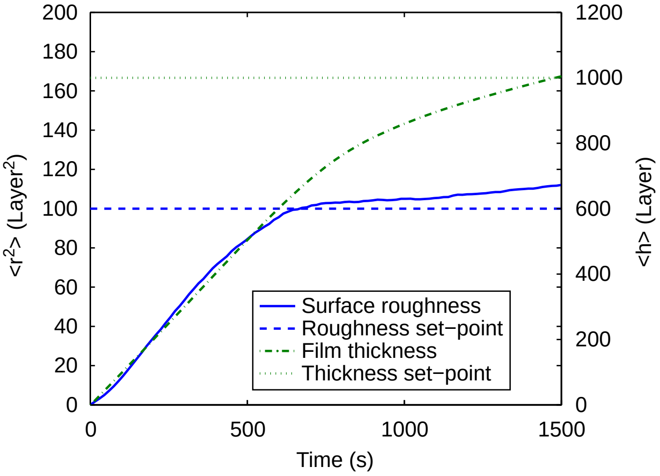

Fig. 8. Profiles of the expected values of surface roughness square (solid line) and of the film thickness (dash-dotted line) under closed-loop operation; roughness control problem with desired minimum of film thickness.

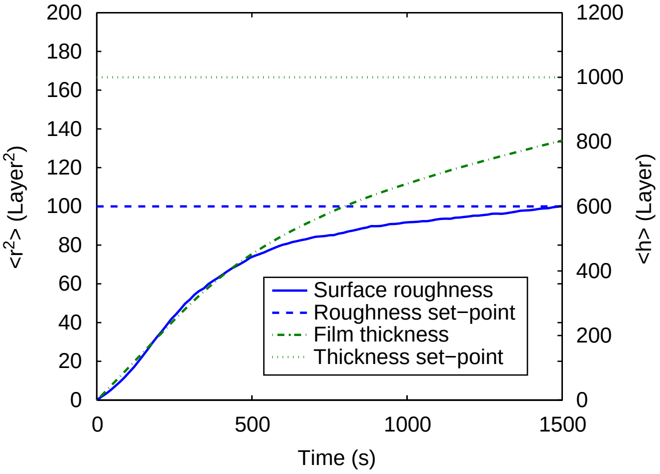

Fig. 9. Profiles of the expected values of surface roughness square (solid line) and of the film thickness (dash-dotted line) under closed-loop operation; roughness control problem without desired minimum of film thickness.

Using the finite-dimensional system of Eq. (27), the expected surface roughness square, $\langle r^2(t)\rangle$, can be approximated with the finite-dimensional state variance as follows:

$$\langle \tilde{r}^2(t)\rangle = \frac{1}{2\pi}\sum_{i=1}^{m}[\langle \alpha_i^2(t)\rangle + \langle \beta_i^2(t)\rangle] \qquad (28)$$

where the tilde symbol in $\langle \tilde{r}^2(t)\rangle$ denotes its association with a finite-dimensional system.

4.2. MPC formulation

We consider the control problem of film thickness, surface roughness and film porosity regulation by using a model predictive control design. The expected values, $\langle h\rangle$, $\langle r^2\rangle$ and ρ, are chosen as the control objectives. The deposition rate is used as the manipulated input. The substrate temperature is fixed at a certain value, T_0, during all closed-loop simulations. We note here that the proposed modeling and control methods do no depend on the specific number of the manipulated variables and can be easily extended to the case of multi-inputs. To account for a number of practical considerations, several constraints are added to the control problem. First, there is a constraint on the range of variation of the deposition rate. This constraint ensures validity of the on-lattice kMC model. Another constraint is imposed on the rate of change of the deposition rate to account for actuator limitations. The control action at time t is obtained by solving a finite-horizon optimal control problem.

The cost function in the optimal control problem includes penalty on the deviation of $\langle r^2 \rangle$ and ρ from their respective set-point values. Since the manipulated variable is the deposition rate and the film deposition process is a batch operation (i.e., the film growth process is terminated within a certain time), a desired minimum of the film thickness is also required to prevent an undergrown thin film at the end of the deposition process. The minimal film thickness is regarded as the set-point value of the film thickness in the MPC formulation, i.e., the deviation of the film thickness from the minimum is included in the cost function. However, only the negative deviation (when the film thickness is less than the minimum) is counted; no penalty is imposed on the deviation when the thin film exceeds the minimal thickness. Different weighting factors are assigned to the penalties on the deviations of the surface roughness and of the film SOR (and of the film thickness as well). Relative deviations are used in the formulation of the cost function to make the magnitude of the different terms used in the cost comparable for numerical calculation purposes. The optimization problem is subject to the dynamics of the reduced-order model of surface roughness of Eq. (27), the dynamics of the film thickness of Eq. (15), and the dynamics of the film SOR of Eq. (21). The optimal profile of the deposition rate is calculated by solving a finite-dimensional optimization problem in a receding horizon fashion. Specifically, the MPC problem is formulated as follows:

$$
\begin{aligned}
\min_{W_1,\ldots,W_i,\ldots,W_p} \quad & J=\sum_{i=1}^{p}(q_{r^2,i}F_{r^2,i}+q_{h,i}F_{h,i}+q_{\rho,i}F_{\rho,i})\\
\text{s.t.} \quad & F_{r^2,i}=\left[\frac{r_{set}^2-\langle \tilde{r}^2(t_i)\rangle}{r_{set}^2}\right]^2\\
& F_{h,i}=\begin{cases}\left[\dfrac{h_{min}-\langle \bar{h}(t_i)\rangle}{h_{min}}\right]^2, & h_{min}>\langle \bar{h}(t_i)\rangle\\[2ex] 0, & h_{min}\leq \langle \bar{h}(t_i)\rangle\end{cases}\\
& F_{\rho,i}=\left[\frac{\rho_{set}-\rho(t_i)}{\rho_{set}}\right]^2\\
& \langle \alpha_n^2(t_i)\rangle=\frac{\sigma^2}{2\nu n^2}+\left(\langle \alpha_n^2(t_{i-1})\rangle-\frac{\sigma^2}{2\nu n^2}\right)e^{-2\nu n^2\varDelta}\\
& \langle \beta_n^2(t_i)\rangle=\frac{\sigma^2}{2\nu n^2}+\left(\langle \beta_n^2(t_{i-1})\rangle-\frac{\sigma^2}{2\nu n^2}\right)e^{-2\nu n^2\varDelta}\\
& \langle \bar{h}(t_i)\rangle=\langle \bar{h}(t_{i-1})\rangle+r_h\varDelta\\
& \rho(t_i)=\frac{\{\rho(t_{i-1})\langle \bar{h}(t_{i-1})\rangle+r_h[\rho^{ss}\varDelta+(\rho^{ss}-\rho(t_{i-1}))\tau(e^{-\varDelta/\tau}-1)]\}}{\langle \bar{h}(t_{i-1})\rangle+r_h\varDelta}\\
& W_{min}<W_i<W_{max}, \quad \left|\frac{W_{i+1}-W_i}{\varDelta}\right|\leq L_W\\
& n=1,2,\ldots,m, \quad i=1,2,\ldots,p
\end{aligned}
\tag{29}
$$

where t is the current time, $\varDelta$ is the sampling time, p is the number of prediction steps, $p\varDelta$ is the specified prediction horizon, t_i, $i=1,2,\ldots,p$, is the time of the ith prediction step ($t_i{=}t{+}i\varDelta$), respectively, W_i, $i{=}1,2,\ldots,p$, is the deposition rate at the ith step ($W_i{=}W(t{+}i\varDelta)$), respectively, $q_{r^2,i}$, $q_{h,i}$ and $q_{\rho,i}$, $i{=}1,2,\ldots,p$, are the weighting penalty factors for the deviations of $\langle r^2 \rangle$ and ρ from their respective set-points r_{set}^2 and ρ_{set}, and $\langle \bar{h} \rangle$ from its desired minimum, h_{min}, at the ith prediction step, W_{min} and W_{max} are the lower and upper bounds on the deposition rate, respectively, and L_W is the limit on the rate of change of the deposition rate. Note that we choose $\langle \bar{h} \rangle$, r_h and $\rho(t_0)$ to replace H, r_H and ρ_{d0} in the MPC formulation of Eq. (29), respectively.

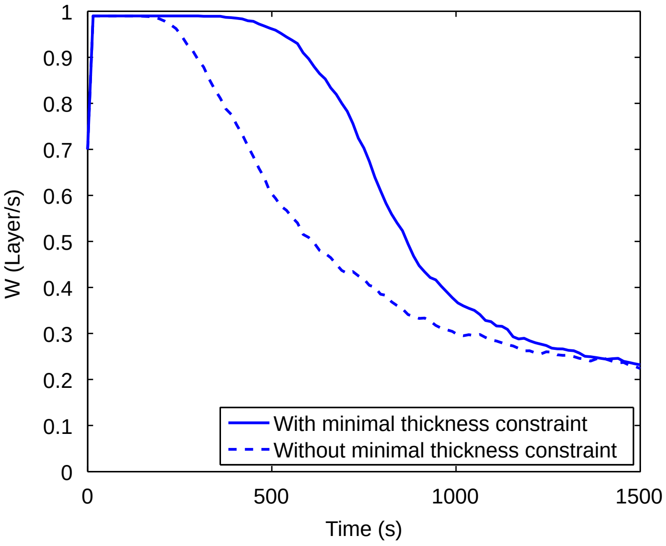

Fig. 10. Profiles of the expected values of deposition rate under closed-loop operation with (solid line) and without (dashed line) desired minimum of film thickness; roughness control problem.

The optimal set of control actions $(W_1, W_2, \ldots, W_p)$, is obtained from the solution of the multi-variable optimization problem of Eq. (29), and only the first value of the manipulated input trajectory, W_1, is applied to the deposition process from time t until the next sampling time, when new measurements are received and the MPC problem of Eq. (29) is solved for the computation of the next optimal input trajectory.

The dependence of the model parameters, r_h, ν, σ^2, ρ^{ss} and τ, on the deposition rate, W, is used in the formulation of the model predictive controller of Eq. (29). The parameters estimated under time-invariant operating conditions are suitable for the purpose of MPC design because the control input in the MPC formulation is piecewise constant, i.e., the manipulated deposition rate remains constant between two consecutive sampling times, and thus, the dynamics of the microscopic process can be predicted using the dynamic models with estimated parameters.

5. Simulation results

In this section, the proposed model predictive controller of Eq. (29) is applied to the kMC model of the thin film growth process described in Section 2. The value of the deposition rate is obtained from the solution of the problem of Eq. (29) at each sampling time and is applied to the closed-loop system until the next sampling time. The optimization problem in the MPC formulation of Eq. (29) is solved via a local constrained minimization algorithm using a broad set of initial guesses. Since the state variables of the system are accessed or measured only at the sampling times in the closed-loop simulations, no statistical information, e.g., the expected complete film SOR, is available for feedback control. Thus, instantaneous values of the surface height profile and film SOR are used as the initial conditions for the dynamic models in the MPC formulation of Eq. (29).

The desired values (set-point values) in the closed-loop simulations are $r_{set}^2=100$ layer^2 and $\rho_{set}=0.96$, with a desired minimum of film thickness of $h_{min}=1000$ layers. The substrate temperature is

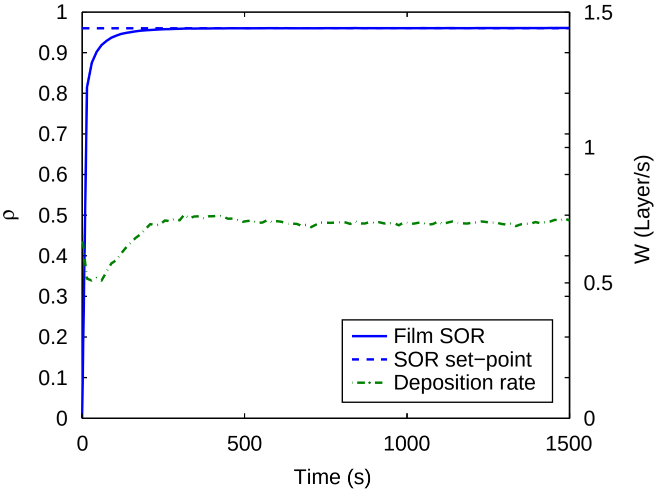

Fig. 11. Profiles of the expected values of film SOR (solid line) and of the deposition rate (dash-dotted line) under closed-loop operation; porosity-only control.

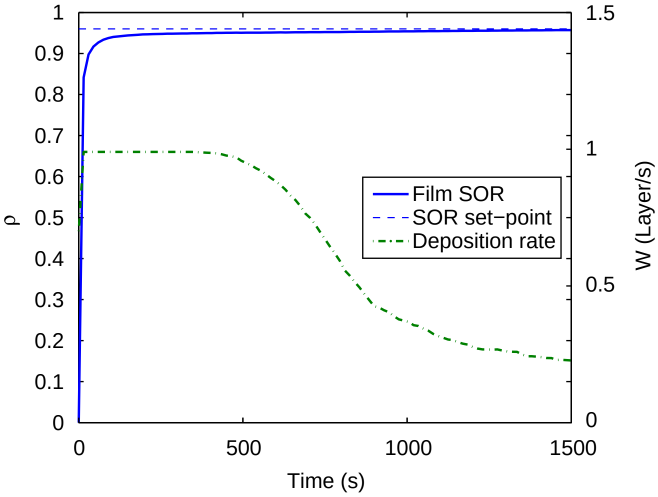

Fig. 13. Profiles of the expected values of film SOR (solid line) and of the deposition rate (dash-dotted line) under closed-loop operation; simultaneous regulation of film thickness, roughness and porosity.

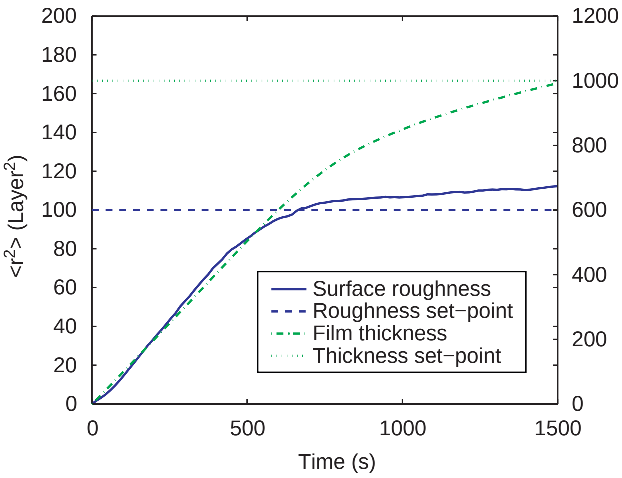

Fig. 12. Profiles of the expected values of surface roughness square (solid line) and of the film thickness (dash-dotted line) under closed-loop operation; simultaneous regulation of film thickness, roughness and porosity.

fixed at 850 K and the initial deposition rate is 0.2 layer/s. The variation of deposition rate is from 0.1 to 1.0 layer/s. The maximum rate of change of the deposition rate is $L_W = 10$ layer/s^2. All penalty factors, $q_{r^2,i}$, $q_{h,i}$ and $q_{\rho,i}$, are set to be either zero or one. The number of prediction steps is set to be $p = 5$. The prediction horizon of each step is fixed at $\Delta = 200$ s. The time interval between two samplings is 5 s. The computational time that is used to solve the optimization problem with the current available computing power is negligible (within 10 ms) with respect to the sampling time interval. The closed-loop simulation duration is 1500 s. All expected values are obtained from 1000 independent simulation runs.

5.1. Regulation of surface roughness with constrained film thickness

Closed-loop simulations of separately regulating film surface roughness with desired minimum of film thickness (roughness control problem) are first carried out. In these control problems, the control objective is to regulate the expected surface roughness square to the desired value (100 layer^2) with a desired minimum of expected film thickness (1000 layers). Thus, the cost functions of these problems contain penalties on the deviations of the expected surface roughness square from the set-point value and of the expected film thickness from its desired minimum value.

Fig. 8 shows the closed-loop simulation results of the roughness–thickness control problem. From Fig. 8, it can be seen that the model predictive controller drives the expected surface roughness square close to the desired value, 100 layer^2, at the end of the simulation. However, due to the existence of desired minimum of film thickness, 1000 layers, the controller computes a higher deposition rate, and thus, it results in a higher expected surface roughness square at the end of the closed-loop simulation. The effect of the minimum of film thickness can be observed by comparing Fig. 8 to Fig. 9, which shows the closed-loop simulation results without desired minimum of film thickness. It can be clearly seen that, without penalty on the deviation of film thickness, the expected surface roughness square approaches the set-point value at the end of the simulation, while the expected film thickness falls under the desired minimum. Fig. 10 shows the comparison between the profiles of deposition rate with and without desired minimum of film thickness included in the cost function. In Fig. 10, it can be seen that the thickness constraint results in a higher deposition rate so that the desired minimum of film thickness can be achieved at the end of the closed-loop simulations.

5.2. Regulation of film porosity by manipulating deposition rate

In this subsection, film SOR is the control objective (porosity control problem). In the porosity control problem, the cost function in the MPC formulation includes only penalty on the deviation of the film SOR from the set-point value, 0.96. Fig. 11 shows the evolution profile of the film SOR from the closed-loop simulation of the porosity control problem. The model predictive controller successfully drives the expected film SOR to the set-point value and stabilizes it at the steady state. There is no offset from the set-point at large times compared to the closed-loop simulation results under a model predictive controller that utilizes a deterministic linear ODE model for the film SOR (Hu et al., 2009a). The elimination of offset demonstrates that the dynamic models of Eqs. (21) and (22), which are postulated in Section 3.2, are suitable for the purpose of porosity control. The corresponding profile of the deposition rate W is also shown in Fig. 11 (dash-dotted line).

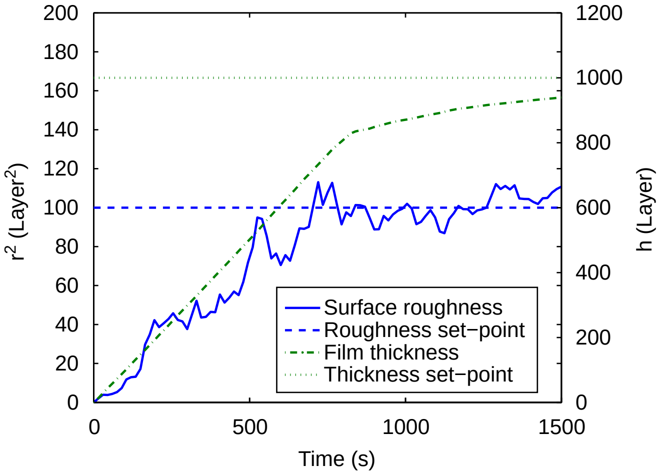

Fig. 14. Profiles of the instantaneous values of surface roughness square (solid line) and of the film thickness (dash-dotted line) under closed-loop operation; simultaneous regulation of film thickness, roughness and porosity.

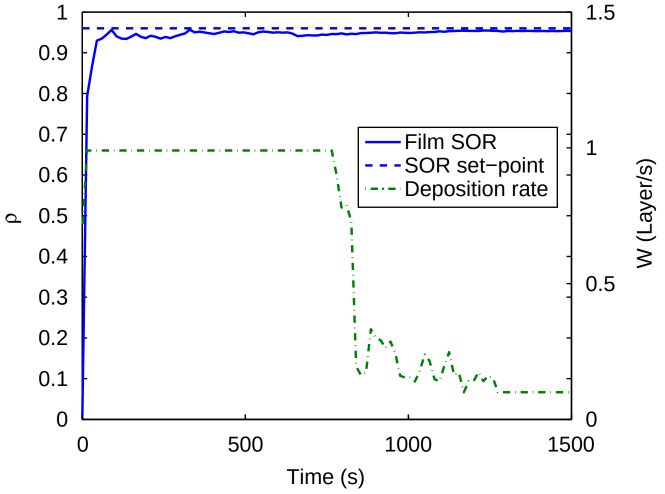

Fig. 15. Profiles of the instantaneous values of film SOR (solid line) and of the deposition rate (dash-dotted line) under closed-loop operation; simultaneous regulation of film thickness, roughness and porosity.

5.3. Simultaneous regulation of surface roughness and film porosity with constrained film thickness

Finally, closed-loop simulations of simultaneous regulation of film thickness, surface roughness and film SOR are carried out. Since the deposition rate is the only manipulated input, the desired values of r^2_{set} and ρ_{set} cannot be achieved simultaneously, i.e., the corresponding adsorption rates for the desired surface roughness and film thickness are not the same. Therefore, a trade-off between the two set-points is made by the controller. Figs. 12 and 13 show the simulation results for this work. The expected values of both surface roughness square and film SOR approach their corresponding set-points with the minimal film thickness being achieved. The simulation profiles of expected surface roughness square and film thickness are close to the profiles from the roughness control problem in Section 5.1. The close profiles are due to the fact that the film SOR is not sensitive to the variation of the deposition rate, and thus, the controller tries to regulate the surface roughness square to its set-point.

Figs. 14 and 15 show the instantaneous values of surface roughness square and film SOR in the closed-loop simulation. The instantaneous values are obtained from a single simulation run, and thus, different runs may result in different profiles. The manipulated deposition rate is also shown in Fig. 15. At the beginning, the controller saturates the deposition rate at the upper bound of 1.0 layer/s to achieve the minimal film thickness. Surface roughness square and film SOR also increase from 0 towards their respective set-points. At about 700 s, surface roughness square reaches its set-point, and soon after that, the optimal deposition rate drops fast close to the lower bound so as to keep the surface roughness square at the set-point and to increase the film thickness close to the minimal value.

6. Conclusions

Distributed control of film thickness, surface roughness and porosity was developed for a porous thin film deposition process. The deposition process includes atom adsorption and migration and was modeled via kinetic Monte Carlo simulation on a triangular lattice. As a batch process, film thickness is an important target variable for the thin film growth process. The deposition rate was thus selected as the manipulated input due to its direct influence on the film thickness. To characterize the evolution of film surface roughness and account for the stochastic nature of the deposition process, a distributed parameter dynamic model was derived to describe the evolution of the surface height profile of the thin film accounting for the effect of deposition rate. The dynamics of film porosity, evaluated as film site occupancy ratio, were described by an ordinary differential equation. The developed dynamic models were then used as the basis for the design of a model predictive control algorithm that includes penalty on the deviation of film thickness, surface roughness and film porosity from their respective set-point values. A reduced-order model of the film surface height was included in the MPC formulation to calculate the prediction of expected surface roughness to meet the requirement of computational efficiency for real-time feedback control calculations. Simulation results demonstrated the applicability and effectiveness of the proposed modeling and control approach in the context of the deposition process under consideration. We found out that the film thickness requirement essentially places a lower bound on the deposition rate, and thus, it limits the range of achievable film porosity.

References

Bohm, M., Demetriou, M.A., Reich, S., Rosen, I.G., 1998. Model reference adaptive control of distributed parameter systems. SIAM Journal on Control and Optimization 36, 33–81.

Christofides, P.D., Armaou, A., Lou, Y., Varshney, A., 2008. Control and Optimization of Multiscale Process Systems. Birkhäuser, Boston.

Christofides, P.D., El-Farra, N.H., 2005. Control of nonlinear and hybrid process systems: designs for uncertainty, constraints and time-delays. Springer, Berlin, German.

Cuerno, R., Makse, H.A., Tomassone, S., Harrington, S.T., Stanley, H.E., 1995. Stochastic model for surface erosion via ion sputtering: dynamical evolution from ripple morphology to rough morphology. Physical Review Letters 75, 4464–4467.

Edwards, S.F., Wilkinson, D.R., 1982. The surface statistics of a granular aggregate. Proceedings of the Royal Society of London Series A—Mathematical Physical and Engineering Sciences 381, 17–31.

Hu, G., Orkoulas, G., Christofides, P.D., 2009a. Modeling and control of film porosity in thin film deposition. Chemical Engineering Science, in press, doi:10.1016/j.ces.2009.05.008.

Hu, G., Orkoulas, G., Christofides, P.D., 2009b. Stochastic modeling and simultaneous regulation of surface roughness and porosity in thin film deposition. Industrial & Engineering Chemistry Research, in press.

Keršulis, S., Mitin, V., 1995. Monte Carlo simulation of growth and recovery of silicon. Material Science & Engineering B 29, 34–37.

Krstic, M., Smyshlyaev, A., 2008. Adaptive control of PDEs. Annual Reviews in Control 32, 149–160.

Lauritsen, K.B., Cuerno, R., Makse, H.A., 1996. Noisy Kuramote–Sivashinsky equation for an erosion model. Physical Review E 54, 3577–3580.

Levine, S.W., Clancy, P., 2000. A simple model for the growth of polycrystalline Si using the kinetic Monte Carlo simulation. Modelling and Simulation in Materials Science and Engineering 8, 751–762.

Lou, Y., Christofides, P.D., 2003a. Estimation and control of surface roughness in thin film growth using kinetic Monte-Carlo models. Chemical Engineering Science 58, 3115–3129.

Lou, Y., Christofides, P.D., 2003b. Feedback control of growth rate and surface roughness in thin film growth. A.I.Ch.E. Journal 49, 2099–2113.

Lou, Y., Christofides, P.D., 2005. Feedback control of surface roughness using stochastic PDEs. A.I.Ch.E. Journal 51, 345–352.

Lou, Y., Hu, G., Christofides, P.D., 2008. Model predictive control of nonlinear stochastic partial differential equations with application to a sputtering process. A.I.Ch.E. Journal 54, 2065–2081.

Mayne, D.Q., Rawlings, J.B., Rao, C.V., Scokaert, P.O.M., 2000. Constrained model predictive control: stability and optimality. Automatica 36, 789–814.

Ni, D., Christofides, P.D., 2005. Multivariable predictive control of thin film deposition using a stochastic PDE model. Industrial & Engineering Chemistry Research 44, 2416–2427.

Reese, J.S., Raimondeau, S., Vlachos, D.G., 2001. Monte Carlo algorithms for complex surface reaction mechanisms: efficiency and accuracy. Journal of Computational Physics 173, 302–321.

Siettos, C.I., Armaou, A., Makeev, A.G., Kevrekidis, I.G., 2003. Microscopic/stochastic timesteppers and "coarse" control: a kMC example. A.I.Ch.E. Journal 49, 1922–1926.

Varshney, A., Armaou, A., 2005. Multiscale optimization using hybrid PDE/kMC process systems with application to thin film growth. Chemical Engineering Science 60, 6780–6794.

Varshney, A., Armaou, A., 2008a. Low-order ode approximations and receding horizon control of surface roughness during thin-film growth. Chemical Engineering Science 63, 1246–1260.

Varshney, A., Armaou, A., 2008b. Reduced order modeling and dynamic optimization of multiscale PDE/kMC process systems. Computers & Chemical Engineering 32, 2136–2143.

Villain, J., 1991. Continuum models of crystal growth from atomic beams with and without desorption. Journal de Physique I 1, 19–42.

Vlachos, D.G., Schmidt, L.D., Aris, R., 1993. Kinetics of faceting of crystals in growth, etching, and equilibrium. Physical Review B 47, 4896–4909.

Vvedensky, D.D., Zangwill, A., Luse, C.N., Wilby, M.R., 1993. Stochastic equations of motion for epitaxial growth. Physical Review E 48, 852–862.

Wang, L., Clancy, P., 1998. A kinetic Monte Carlo study of the growth of Si on Si(1 0 0) at varying angles of incident deposition. Surface Science 401, 112–123.

Wang, L., Clancy, P., 2001. Kinetic Monte Carlo simulation of the growth of polycrystalline Cu films. Surface Science 473, 25–38.

Yang, Y.G., Hass, D.D., Wadley, H.N., 2005. Porosity control in zig-zag vapor-deposited films. Thin Solid Films 471, 1–11.

Yang, Y.G., Johnson, R.A., Wadley, H.N., 1997. A Monte Carlo simulation of the physical vapor deposition of nickel. Acta Materialia 45, 1455–1468.

Zhang, P., Zheng, X., Wu, S., Liu, J., He, D., 2004. Kinetic Monte Carlo simulation of Cu thin film growth. Vacuum 72, 405–410.

Ziff, R.M., Gulari, E., Barshad, Y., 1986. Kinetic phase transitions in an irreversible surface-reaction model. Physical Review Letters 56, 2553–2556.